$CDCl_3$ in an NMR tube. After degassing, the solution was sealed under hydrogen and placed at room temperature. For comparison, a second tube was prepared containing only complex IV (14 mg, 0.022 mmol) dissolved in 0.5 mL of $CDCl_3$. This solution was also degassed and sealed under hydrogen. after 6 h at room temperature, the NMR spectrum of the first solution showed that the pyridine had been converted to pyridinium ion and that the molybdenum species consisted of the methanedithiolate bridged dimer and complex V. A broad peak at 6.17 ppm was also present, but disappeared after several days. No further reaction took place over the period of 1 week-no SH resonance were observed. The blue-green solution was then placed at 40 °C. After 2 weeks, reaction was complete to give $(CpMo\text{-}\mu\text{-}S)_2S_2CH_2$ and ethylbenzene with some insoluble brown solids.

After 6 h at room temperature, the NMR spectrum of the second tube showed broadened resonances of the starting complex IV and very small amounts of the methanedithiolae bridged dimer and of complex V. Heating the solution at 40 °C for 2 weeks gave the same products as observed above.

Reaction of $(CpMo)_2(S_2CH_2)(\mu\text{-}SCH(Me)Ph)_2$, V, with Hydrogen. Complex V (10 mg, 0.015 mmol) was dissolved in 0.5 mL of deuteriochloroform in an NMR tube. The solution was degassed, sealed under 450 mm of hydrogen, and placed at 40 °C. Hydrogenolysis proceeded to 62% completion in 6 days to give ethylbenzene and $(CpMo\text{-}\mu\text{-}S)_2S_2CH_2$. The reaction slowly went to completion after 1 month.

Acknowledgment. We thank the U.S. Department of Energy, Office of Basic Energy Sciences, Chemical Sciences Division, and the National Science Foundation. M.R.D. is grateful for a Guggenheim Fellowship, 1984-85, and a Dreyfus Fellowship, 1981-86.

Supplementary Material Available: Anisotropic temperature factors (1 page); calculated and observed structure factors for the crystal structure of I (21 pages). Ordering information can be found on any current masthead page.

Topological Enhancement of Basicity: Molecular Structure and Solution Study of a Monoprotonated Catenand

Michèle Cesario,[†] Christiane O. Dietrich,*[‡] André Edel,[‡] Jean Guilhem,[†] Jean-Pierre Kintzinger,*[§] Claudine Pascard,*[†] and Jean-Pierre Sauvage*[‡]

Contribution from the Laboratoire de Cristallochimie, Institut de Chimie des Substances Naturelles, C.N.R.S., 91190 Gif-sur-Yvette, France, Laboratoire de Chimie Organo-Minérale, Institut de Chimie, B.P. 296/R8, 67008 Strasbourg Cédex, France, and Laboratoire de Chimie Organique Physique, Institut Le Bel, 67000 Strasbourg, France. *Received April 2, 1986*

Abstract: The molecular structure of a proton catenate has been determined by X-ray crystallography. It is very similar to that of the copper(I) catenate, the two 2,9-diphenyl-1,10-phenanthroline fragments being entwined, contrary to the situation in the free ligand. A detailed ^1H NMR study in solution has been performed, demonstrating the entwined topography of the system either for the mono- or the diprotonated molecule. The basicity of the catenand is several orders of magnitude higher than that of its open chain analogue, this enhancement of basicity being due to topological factors only.

Interlocked macrocyclic ligands represent a new class of coordinating molecules whose first member **1** has recently been synthesized[1] (see Chart I). The catenand **1** is able to coordinate a large variety of transition metals, low oxidation states being highly stabilized.[2-5] Other species like Li^+ form complexes with **1** in which the two 2,9-diphenyl-1,10-phenanthroline (dpp) fragments are entwined while coordinating to the cation,[5] such a topography being typical of all the catenates $\mathbf{1}.M^{n+}$ prepared up to now. We wish to report that H^+ leads also to the same type of geometry, either in the solid state—as shown by X-ray crystallography—or in solution. In addition, for topological reasons, the monoprotonated catenand is surprisingly stabilized with respect both to the free ligand and to the diprotonated species. For comparison purposes, protonation studies on the open chain analogue **2** have also been performed.

Experimental Section

Preparation of the Proton Catenate. **1**[1] (50 μmol, 57 mg) is dissolved in 10 mL of CH_2Cl_2, and 4.9 μmol (4.9 mg) of $HClO_4$ in a mixture of CH_3OH and H_2O (4:1) is added at room temperature with stirring. Instantaneously, a bright lemon yellow color appears, indicating a fast protonation reaction of **1**. After standing overnight, the solvent is pumped off under vacuum. The solid residue is redissolved in CH_2Cl_2 (10 mL), and the organic phase is washed 3 times with 10 mL of distilled water. The organic layer is dried over $MgSO_4$, filtered, and evaporated. The yellow solid obtained is pure $[\mathbf{1}\cdot H^+][ClO_4^-]\cdot 2H_2O$ (64 mg, quantitative yield). The compound might be recrystallized from CH_2Cl_2-benzene, affording an analytical sample.

Analytical and spectroscopic data for $[\mathbf{1}\cdot H^+][ClO_4^-]\cdot 2H_2O$ (mp 226-228 °C). Anal. Calcd for $C_{68}H_{73}H_4O_{18}Cl$: C, 64.32; H, 5.67; N, 4.41. Found: C, 64.80; H, 5.69; N, 4.49. Electronic spectrum (CH_2Cl_2) λ_{max} in nm (ϵ) = 270 nm (57 000), 300 (48 000), and shoulder at 340 (34 000).

Incidently, the same compound was made from **1** and $Ni(ClO_4)_2\cdot 6H_2O$ in excess in CH_2Cl_2-CH_3OH (1:1). After an identical workup as that described above, a quantitative yield of $[\mathbf{1}\cdot H^+][ClO_4^-]$, $2H_2O$ is also obtained.

X-ray Study. Crystals were grown from CH_2Cl_2-benzene as bright yellow prisms: $[C_{68}H_{69}N_4O_{12}]^+[ClO_4^-]$, $2C_6H_6$; monoclinic, $P2_1/c$ a = 14.539 (9) Å, b = 20.406 (14) Å, c = 24.852 (17) Å, β = 103.86° (10), U = 7158 Å^3, Z = 4.

The 5048 observed data were collected on an automatic Philips diffractometer. The structure was solved by direct methods using a local program.[6] Two benzene molecules were located on the asymmetric unit. All H atoms appeared on difference Fourier maps. Refinement with anisotropic thermal parameters for heavy atoms and isotropic for H atoms, led to an R factor of 7.0% (R_w = 6.2%). First peak on the last difference series was 0.25 e high.

NMR Spectroscopy. Spectra were obtained by using a Bruker WP-200 operating at a ^1H resonance frequency of 200.13 MHz. Low-

[†] Laboratoire de Cristallochimie.
[‡] Laboratoire de Chimie Organo-Minérale.
[§] Laboratoire de Chimie Organique Physique.

(1) Dietrich-Buchecker, C. O.; Sauvage, J. P.; Kern, J. M. *J. Am. Chem. Soc.* **1984**, *106*, 3043.
(2) Dietrich-Buchecker, C. O.; Sauvage, J. P.; Kintzinger, J. P. *Tetrahedron Lett.* **1983**, *46*, 5095.
(3) Dietrich-Buchecker, C. O.; Kern, J. M.; Sauvage, J. P. *Chem. Commun.* **1985**, 760.
(4) Sauvage, J. P. *Nouv. J. Chim.* **1985**, *9*, 299.
(5) Dietrich-Buchecker, C. O.; Kern, J. M.; Sauvage, J. P., manuscript in preparation.
(6) Riche, C. 7th European Crystallographic Meeting, Jerusalem, 1982; *Chem. Abstr.* p 25.

0002-7863/86/1508-6250$01.50/0

Chart I

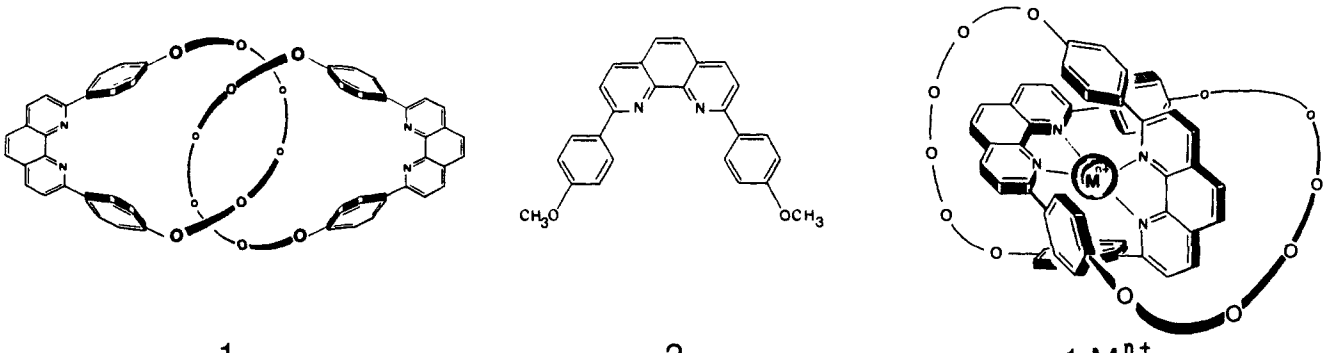

1 2 1.M^{n+}

temperature measurements were performed by using a Bruker B-VT 1000 variable temperature unit. The internal lock signal was CD_2Cl_2. Titration studies were made in CD_2Cl_2/CD_3CN mixtures (70/30), **1** or **2** solutions being $1-6 \times 10^{-3}$ M. The buffers were $4-7 \times 10^{-2}$ M. The following pK_a values were assumed for the various acido–basic couples used (in H_2O, at 25 °C): base, pK_a; 3-chloropyridine, 2.84;[7a] pyridine, 5.45;[7b] 2,6-lutidine, 6.60;[7c] 2.4,6-collidine, 7.43;[7c] morpholine, 8.7.[7b]

Discussion

The molecular structure of $[\mathbf{1}\cdot H^+][ClO_4^-]$ is represented in Figure 1. For comparison, the structure of $[\mathbf{1}\cdot Cu^+][BF_4^-]$[8] is also shown. The shape of $\mathbf{1}\cdot H^+$ is drastically different from that of the free ligand **1**, whose crystallographic study has recently been reported.[8] The structure of $\mathbf{1}\cdot H^+$ indicates that this compound is a *proton catenate*: the two macrocycles are interlocked, and the two dpp fragments are entwined. The molecular topography of $\mathbf{1}\cdot H^+$ is strikingly similar to that of the copper(I) catenate $\mathbf{1}\cdot Cu^+$; the two phenanthroline rings are facing each other with a dihedral angle of 61°.

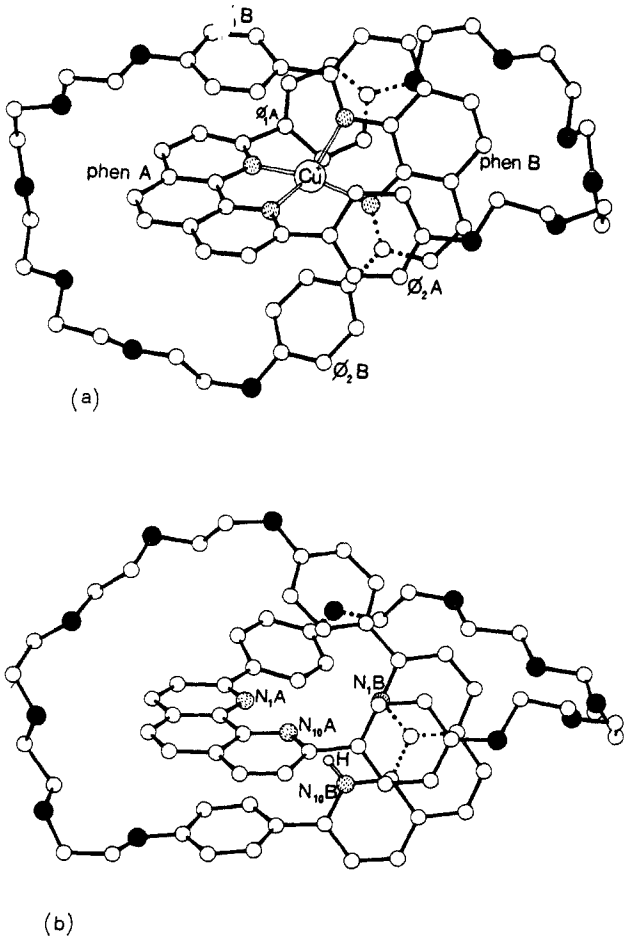

Figure 1. Molecular structure of (a) the copper(I) catenate $\mathbf{1}\cdot Cu^+$ and (b) the proton catenate $\mathbf{1}\cdot H^+$.

Table I. Some Relevant Geometrical Features of the Proton and Copper(I) Catenates

	$\mathbf{1}\cdot Cu^+$	$\mathbf{1}\cdot H^+$
Phenanthrolines		
angle phen A, phen B	61°	62°
angles with phenyl rings:		
phen A, Ph_1 A	55	23
phen A, Ph_2 A	52	63
phen B, Ph_1 B	27	27
phen B, Ph_2 B	58	54
Interaction between Aromatic Rings		
angles (shortest dist in Å)		
phen A, Ph_2 B	6 (3.16–3.5)	10 (3.36–3.6)
phen B, Ph_2 A	11 (3.2–3.3)	5 (3.3–3.5)
Ph_1A, Ph_1B	5 (3.4)	23 (3.3–4.2)
Pentoxyethylene Fragments		
planeity A	bent	±1.4 Å
planeity B	±0.8 Å	±0.7 Å
torsion angles O–C	trans 80%	70%
torsion angles C–C	gauche 80%	50%
Tetrahedron of Nitrogen Atoms: Distances in Å		
N_1A–N_1B	3.71	4.06
N_1A–$N_{10}B$	3.75	3.90
$N_{10}A$–N_1B	3.71	3.60
$N_{10}A$–$N_{10}B$	2.88	3.10

One can notice a particular stacking between a given phenanthroline ring and a phenyl group borne by the other phenanthroline: phen A and phen B are roughly parallel to Ph_2B and Ph_1A, respectively (dihedral angle ~5–10°), as shown in Figure 1.

The internal stacking of the aromatic rings within the two catenates is also nearly the same, with very similar dihedral angles except for a larger deviation from parallelism in $\mathbf{1}\cdot H^+$ than in $\mathbf{1}\cdot Cu^+$. This intramolecular interaction reflects the donor character of the phenyl groups. It also shows that by a **single** protonation **both** phenanthroline nuclei become sufficiently electron acceptor for forming acceptor–donor complexes with the phenyl rings.

Table I lists some important numerical values on the geometry of the two catenates: angles and distances between aromatic rings (phenyl groups and phenanthroline nuclei), planarity of the pentaoxyethylene fragments, torsion angles of the O–C–C–O links, and geometrical feature of the four nitrogen atoms. The latter are the apices of a twisted tetrahedron. In $\mathbf{1}\cdot H^+$, phen B is slightly slid (0.5 Å) with respect to $\mathbf{1}\cdot Cu^+$ so that one of the nitrogen atoms

(7) (a) Brown, H. C.; McDaniel, D. H. *J. Am. Chem. Soc.* **1955**, *77*, 3752. (b) Bruelman, R. J.; Verhoek, F. H. *J. Am. Chem. Soc.* **1948**, *70*, 1401. (c) Gero, A.; Markham, J. J. *J. Org. Chem.* **1951**, *16*, 1835.

(8) Cesario, M.; Dietrich-Buchecker, C. O.; Guilhem, J.; Pascard, C.; Sauvage, J. P. *Chem. Commun.* **1985**, 244.

Table II. ^{1}H NMR Spectra of **1**, **2**, and Their Protonated Forms: δ (ppm) in CD_2Cl_2-CD_3CN (70/30)

compd	$H_{4,7}$	$H_{5,6}$	$H_{3,8}$	H_o	H_m	H_α or CH_3 (J in Hz)	H_ϵ	H_β, H_γ, H_δ
1	8.29	7.77	8.08	8.41	6.99	4.09, t (7.0)	3.62, s	3.5-3.7, m
1·H^+	8.50	7.94	7.68	7.16	6.15	3.93, t (4.5)	3.69, s	3.5-3.7, m
1·H_2^{2+}	8.90	8.33	8.12	7.63	6.55	3.90, t (5.0)	3.63, s	3.5-3.7, m
2	8.30	7.77	8.11	8.40	7.10	3.88, s		
2·H^+	8.81	8.12	8.39	8.25	7.20	3.92, s		

[a] Internal reference $CDHCl_2$ at 5.32 ppm. [b] $H_{5,6}$ leads to a singlet; $H_{3,8}$ and $H_{4,7}$ show an AB pattern (coupling constant $J \sim 8.5$ Hz) whereas H_o and H_m give rise to AA'XX' systems ($J \sim 8.7$ Hz).

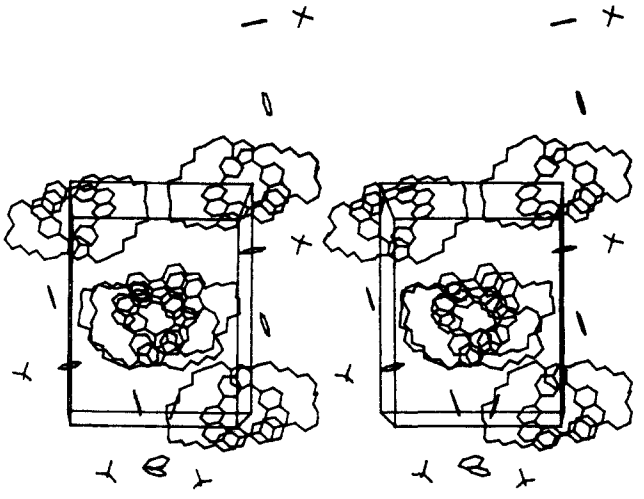

Figure 2. Stereoscopic view of the packing within the crystal of **1**·H^+.

of phen B (N_1B) is located in the plane of phen A (see Figure 1).

The acidic proton borne by phen B is clearly distinguishable on the Fourier difference map. It is accurately located, the covalent N_{10}B–H bond being 0.78 Å long. This bond length is in agreement with that of other N^+–H groups of similar compounds. For instance, the monoprotonated[9,10] and the diprotonated[11] forms of phen (phen = 1,10-phenanthroline) have recently been studied by crystallography. In phen H^+·ClO_4^-, the N^+–H bond length is 0.85 Å[10] whereas it is found to be 0.93 Å in phen H^+·Cl^-, H_2O[9]. In both structures, the acidic hydrogen atom is stabilized by interactions with the anion (ClO_4^-) or H_2O within the crystal lattice. The diprotonated compound phen H_2^{2+}·$2ClO_4^-$, H_2O exhibits a longer N^+–H bond: 1.00–1.02 Å.[11]

The stability of the molecular edifice is ensured by an efficient hydrogen bond formed with one nitrogen site belonging to the other macrocyclic subunit (N_{10}A to H = 2.49 Å), the other nitrogen atom of this same subunit being remote (N_1A to H distance = 3.20 Å). In addition, a short hydrogen bond with the other nitrogen atom of the phenanthroline nucleus bearing the acidic proton is observed (N_1B···H = 2.35 Å). The structure is perfectly ordered, and the complexes are stabilized in the crystal by their own geometries, by the perchlorate anion, and by the two solvate benzene rings. The packing forces influence the molecular assembly within the crystal, as represented in Figure 2.

The ligand **1** is highly adaptable to the complexed species, due to the absence of covalent bond between the two coordinating rings. As a consequence, no thermodynamic selectivity of complexation can be expected with respect to the size of the coordinated moiety. The adaptability of the catenand **1** is due to the ease with which one of the two interlocked rings can undergo translational and rotational motions with respect to the other. **1** is thus drastically different from the other multicyclic systems designed for strong and selective complexation. For instance, cryptands[13] or spherands[14] contain a preformed complexing site whose shape and size is preferentially adapted to a given substrate. With such complexing agents, whose coordinating site is relatively rigid, selectivity is observed. In addition, contrary to **1** and its complexes, the ligand usually has a general shape analogous to that of its coordination products, although in a few examples, considerable swelling of the preexisting molecular cavity by linking of the substrate might take place.[15]

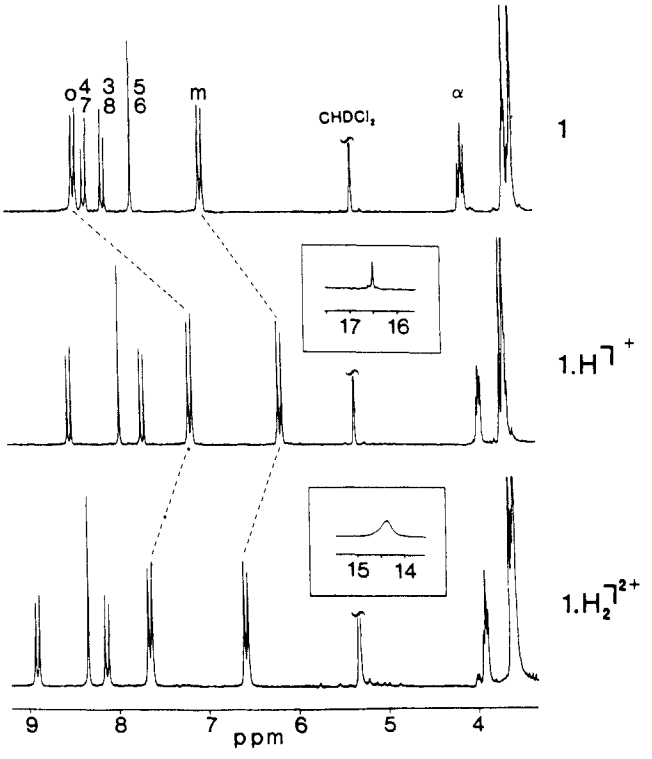

Figure 3. ^{1}H NMR spectra (200 MHz) of the catenand **1** and of its mono- and diprotonated forms. The signals corresponding to the acidic proton(s) of **1**·H^+ and **1**·H_2^{2+} are shown in the respective inserts. The particular signals have been recorded at −70 °C.

NMR studies have been performed in order to show that the solid-state structure of **1**·H^+ also corresponds to the geometry of the molecule in solution and to evaluate the basicity of **1**.

The ^{1}H NMR spectra of **1** and **1**·H^+ are represented in Figure 3. The comparison of both spectra shows that the hydrogen atoms borne by the phenyl rings undergo a strong upfield shift by protonation of **1**. The shielding effect (−1.25 ppm for H_o and −0.85 ppm for H_m, see Table II) is similar to that found in related copper(I) complexes: $(\mathbf{2})_2$·Cu^+[16] and **1**·Cu^+.[2] This shielding arises from the intense ring current effect of the phen nuclei: it clearly

(9) Thevenet, G.; Toffoli, P.; Rodier, N.; Ceolin, R. *Acta Crystallogr., Sect. B: Struct. Crystallogr. Cryst. Chem.* **1977**, *B33*, 2526.
(10) Thevenet, G.; Toffoli, P.; Rodier, N. *Acta Crystallogr., Sect. B: Struct. Crystallogr. Cryst. Chem.* **1978**, *B34*, 2599.
(11) Thevenet, G.; Rodier, N.; Khodadad, P. *Acta Crystallogr., Sect. B: Struct. Crystallogr. Cryst. Chem.* **1978**, *B24*, 2594.
(12) *A Critical Review of Equilibrium Data for Proton and Metal Complexes of 1,10-Phenanthroline, 2,2'-Bipyridyl and Related Compounds*; McBryde, W. A. E., Ed.; Pergamon Press: Oxford, 1978.
(13) Lehn, J. M. *Science (Washington, DC)* **1985**, *227*, 849 and references therein.
(14) Cram, D. J.; Kaneda, T.; Helgeson, R. C.; Lein, G. M. *J. Am. Chem. Soc.* **1979**, *101*, 6752.
(15) Pascard, C.; Riche, C.; Cesario, M.; Kotzyba-Hibert, F.; Lehn, J. M. *Chem. Commun.* **1982**, 557.
(16) Dietrich-Buchecker, C. O.; Marnot, P. A.; Sauvage, J. P.; Kintzinger, J. P.; Maltèse, P. *Nouv. J. Chim.* **1984**, *8*, 573.

demonstrates that the two dpp fragments are entwined around the proton, the two phenyl groups of one dpp being located one on either side of the phen plane of the other macrocycle.

The spectrum of the polyoxyethylene link of **1**·H^+ is modified with respect to that of **1** and its transition-metal complexes. The CH_2 groups of the ϵ positions are shifted downfield with respect to the free ligand, but this deshielding effect is not as pronounced for **1**·H^+ as it is for **1**·Cu^+.[2] Such a difference between the proton and copper(I) catenates holds to dissimilarities in their geometries: the pentethyleneoxy fragments of **1**·H^+ are more remote from the phen nuclei than in **1**·Cu^+, making the ϵ hydrogen atoms less exposed to the deshielding effect of the phen plane.

The acidic proton of **1**·H^+ gives a signal integrating for one hydrogen at 17.5 ppm. **1**·H^+ can also be generated in solution by gradual addition of trifluoroacetic acid to a CH_2Cl_2 solution of **1**: 1 equiv of acid is needed in the titration, and the equilibrium between **1** and **1**·H^+ is slow on the NMR time scale.

At room temperature, the signal of the acidic hydrogen of **1**·H^+ is relatively broad ($\Delta_{1/2} \sim 88$ Hz) as well as that of residual water in the solution. An experiment of saturation transfer between both sites (bound H^+ and H_2O in the solvent) shows a slow exchange between those two sites. An upper limit for the exchange rate constant between N^+–H and external H_2O can be obtained from the line width of the H^+ site, neglecting any broadening contribution arising from a ^{14}N to H coupling[17] ($k < 250\ s^{-1}$ and $\Delta G_{293}^{\ddagger} > 14$ kcal·mol^{-1}).

Although in the solid state, the acidic hydrogen atom is located on one of the four nitrogen sites (Figure 1), the ^1H NMR spectrum of **1**·H^+ in CD_2Cl_2 corresponds to a symmetrical species, indicating a fast exchange between the four nitrogen atoms. The NMR spectrum is still that of a symmetrical species at −60°.[18] The chemical shift found for the acidic proton of **1**·H^+ (= 17.5 ppm) should be compared to that of bpy·H^+ (bpy = 2,2′-bipyridine) (= 10.52 ppm).[19] The large downfield shift of the acidic proton might be due to hydrogen bonding or to an additional deshielding effect due to the presence of the second phen.

Titration of **1** by acids has been carried out, showing surprising acido–basic properties for **1**, **1**·H^+, and **1**·H_2^{2+}. Due to the insolubility of **1** in water and hydroxylated solvents, the acid–base equilibria involving **1** and its protonation products have been studied in CD_2Cl_2/CD_3CN (70/30). The first pK_a (**1**·H^+/**1**: pK_1) has been determined by a competition method, in the presence of a large excess of a given base B and its conjugated acid BH^+. In order to estimate this pK_1 value, it is assumed that, for the whole series of nitrogen bases used, the order of basicity is the same in water and in our organic solvent. The knowledge of p$K_{BH^+/B}$, and the measure of the respective concentrations of **1** and **1**·H^+ in the solution lead to an approximate value of pK_1. For instance, in a morpholinium$^+$/morpholine (62/38) buffer (4.4×10^{-2} M in CD_2Cl_2/CD_3CN (70/30); pK = 8.7), the catenand **1** is in equilibrium with its monoprotonated form: $[\mathbf{1}\cdot H^+]/[\mathbf{1}] \doteq 0.94$, as measured by ^1H NMR, giving a calculated value of pK_1 = 8.5. When a reference couple BH^+/B whose pK value exceeds 9.5 is used, the protonated form **1**·H^+ is very minor. On the other hand, if p$K_{BH^+/B} < 7$, **1**·H^+ is the only species detected.

The same type of experiment can be performed on **2**, the open chain analogue of **1**. The following pK value is thus obtained: **2**·H^+/**2**: pK_1 = 5.1. Whereas **2** has a pK_1 value close to that expected for such a substituted phenanthroline,[12] pK_1 of the catenand is surprisingly high. In another set of experiments, on a sample containing both **1** and **2** in the presence of morpholine, it is possible by titration with CF_3COOH to reach a point where **1** is more than 90% protonated whereas **2** is present as the free base (more than 95%) demonstrating that the pK difference for those two compounds is indeed of the order of 3.

In addition, under the conditions used in NMR spectroscopy, there is no indication for the formation of species analogous to **1**·H^+ and containing two entwined dap molecules around a proton ((**2**)$_2H^+$) (see Table I). Interestingly, the electronic properties and the shape of the coordinating site in **1** or **2** are identical.[2,5] Consequently, the **high basicity of 1 originates mainly from the topology of the molecule**: ΔpK = pK_1(**1**·H^+/**1**) − pK_1(**2**·H^+/**2**) = 3.4. The 2500 factor found between the basicity constants of **1** and dap is also understandable when considering the molecular arrangement of their protonation products: **2**·H^+ is a normal phenanthrolinium ion, but **1**·H^+ is highly stabilized by intramolecular stacking. The acceptor–donor interaction occurring between the phenanthroline nuclei and the phenyl rings accounts for the noticeable stabilization of the catenates in general and of **1**·H^+ in particular.

The exceptional stability of the proton catenate is also evidenced by the low value of the second pK_a: in CD_2Cl_2/CD_3CN (70/30), CF_3COOH is not acidic enough to fully protonate **1**·H^+, even when used in excess. However, perchloric acid reacts quantitatively with **1**·H^+, yielding a diprotonated catenate **1**·H_2^{2+} in which the two dpp subunits are still entwined. By considering approximate values for the pK_a's of CF_3COOH (0.23[20]) and $HClO_4$ (−1.5[21]), an approximate value for the acidity constant of **1**·H_2^{2+} can be obtained

$$\mathbf{1}\cdot H_2^{2+} \rightleftharpoons \mathbf{1}\cdot H^+ + H^+ \qquad pK_2 \sim 1.5$$

The low pK_a value has been confirmed by taking the spectrum of **1** in a 3-chloropyridine buffer at pH 2.84. In this medium, **1**·H^+ and **1**·H_2^{2+} are both present, their acidic protons undergoing fast exchange. The measured chemical shift (17.4 ppm) is intermediate between those corresponding to the mono- and the diprotonated species. It leads to a **1**·H^+/**1**·H_2^{2+} ratio of 97/3 from which a pK_2 value of 1.3 can be deduced.

The entwined topography of **1**·H_2^{2+} is clearly demonstrated by ^1H NMR studies. The spectrum of **1**·H_2^{2+} is shown in Figure 3. The two acidic protons of **1**·H_2^{2+} give rise to a signal at δ = 14.4 ppm. Analogously to **1**·H^+, the spectrum of diprotonated species shows high field H_o and H_m signals (see Table II), characteristic of the catenate structure: the two phenyl rings of the same dpp are located one on either side of the phen nucleus of the other dpp moiety. It is remarkable that, by a second protonation of **1**, one does not loose the entwined geometry with subsequent formation of a diprotonated species whose geometry would be close to that of the free catenand.[8] Such an arrangement would allow the two phen coordination sites—and consequently the two N^+–H groups—to be ~12 Å apart.[8] Clearly, disentangling of the two dpp fragments of **1**·H_2^{2+} would be much more favorable than the actual geometry with respect to electrostatic repulsion between the two N^+–H charges. On the other hand, the acceptor–donor interaction occurring in the catenate structure between phenyl groups and phen rings greatly stabilizes the molecular edifice. Indeed, this interaction is strong enough to force the second proton to come close to the first one. The size of such a stabilization effect can be roughly estimated by comparing the pK_2 value actually measured to that expected if no acceptor–donor complexation was taking place. In this case, the two dpp fragments would be independent, and their basicities would be identical with that of **2**.

$$\mathbf{1}\cdot H_2^{2+}\text{: } pK_2 \sim 1.5$$

$$\mathbf{2}\cdot H^+\text{: } pK = 5.1$$

The topological factor (interlocking of the two rings) whose effect is to favor the particular topography of the proton catenate **1**·H^+ with respect to a second protonation is thus $\sim 10^4$, corresponding to a stabilization energy $\Delta G° \sim -5.4$ kcal·mol^{-1}.

It is noteworthy that the entwined arrangement of the two dpp subunits occurring by protonation is favored for electronic reasons. Since a phen·H^+ grouping is more electron acceptor than the unprotonated species, the charge transfer taking place between the phenyl rings (donors) and the acceptors will be more pro-

(17) Kintzinger, J. P.; Lehn, J. M. *Mol. Phys.* **1968**, *14*, 133.
(18) At this temperature, the H_o and H_m signals are significantly broadened, as for other catenates, indicating that some conformational processes are slowed down.
(19) Pawlak, Z. *Roczniki Chem.* **1973**, *47*, 347.
(20) Henne, A. L.; Fox, C. J. *J. Am. Chem. Soc.* **1951**, *73*, 2325.
(21) Haase, R.; Ducker, K. H.; Kuppers, H. A. *Chem. Ber.* **1965**, *69*, 97.

nounced after protonation, making the molecular edifice stable and rigid, whereas the free catenand is highly flexible. Interestingly, the same phenomenon holds for $1{\cdot}H_2^{2+}$, the electrostatic repulsion between the two bound protons being compensated by a stronger acceptor–donor interaction. It might even be predicted that with highly positively charged species as complexed moieties, a strong additional stabilization (energy and rigidity) arising from intramolecular charge transfer should be observed.

Conclusion

The catenand **1** undergoes a complete rearrangement by protonation, $1{\cdot}H^+$ and $1{\cdot}H_2^{2+}$ being proton catenates whose dpp fragments are entwined around the proton(s). The special shape of $1{\cdot}H^+$, as studied by X-ray crystallography and ^1H NMR, is highly stabilized with respect to the acyclic analogue **2**. This topological effect is very effective both for the mono- and the diprotonated species. An illustration of the catenand effect is found in the unusually high basicity observed for phenanthroline sites. Although the catenand **1** is a flexible molecular system, for which each ring is able to glide freely within the other, the molecular edifice obtained after protonation is rigid and surprisingly stable. An unexpected but strong contribution to the stabilization originates in a charge-transfer interaction. This interaction is remote from the protonation site, but its strength is much dependent on the protonation degree. Such an example, for which simple protonation processes entirely govern the geometry of the molecular system as well as intramolecular interactions, might be generalized to other cases more relevant to biological problems.

Registry No. $1{\cdot}HClO_4$, 103733-28-4.

Structures of Alumina-Supported Osmium Clusters ($HOs_3(CO)_{10}\{OAl\}$) and Complexes ($Os^{II}(CO)_{n=2or3}\{OAl\}_3$) Determined by Extended X-ray Absorption Fine Structure Spectroscopy

F. B. M. Duivenvoorden,† D. C. Koningsberger,*† Y. S. Uh,‡ and B. C. Gates‡

Contribution from the Laboratory for Inorganic Chemistry and Catalysis, Department of Chemical Technology, Eindhoven University of Technology, 5600 MB Eindhoven, The Netherlands, and Center for Catalytic Science and Technology, Department of Chemical Engineering, University of Delaware, Newark, Delaware 19716. *Received November 19, 1985*

Abstract: EXAFS measurements have been carried out with $Os_3(CO)_{12}$, the supported cluster $HOs_3(CO)_{10}\{OAl\}$ prepared by reaction of $Os_3(CO)_{12}$ with γ-Al_2O_3, and the supported sample after decomposition in He at 150 °C. The data were analyzed by applying phase- and/or amplitude-corrected Fourier transforms together with the difference file technique for reliable separation of the various contributions in the composite EXAFS spectrum. Phases and backscattering amplitudes were obtained from reference compounds; the reference for the Os—C≡O moiety was derived from $Os_3(CO)_{12}$. The results are consistent with the surface structure $HOs_3(CO)_{10}\{OAl\}$, postulated previously. The Os—Os and Os—C≡O coordination distances in the cluster do not change upon reaction of $Os_3(CO)_{12}$ with the support; two osmium atoms of the cluster are coordinated to a bridging oxygen anion at an average Os—O distance of 2.16 Å. After decomposition of the supported cluster, the Os—Os oscillations disappeared from the spectrum. The average Os—C≡O coordination number for the osmium ion (valence state presumably +2) was found to be 2.8. The osmium ion was surrounded by three support oxygen neighbors at an average distance of 2.17 Å.

Introduction

Supported metal catalysts used in many large-scale processes consist of small (~10–1000 Å) aggregates or crystallites of metal dispersed on high-surface-area metal–oxide supports. Since the metal aggregates are nonuniform in size, shape, and catalytic properties, the best attainable relations between structure and catalytic performance have been based on the average structural properties which are inferred—sometimes tenuously—from indirect structure probes. Only for very small aggregates of structurally simple supported metals are structures well defined; X-ray absorption spectroscopy, combined with other physical methods, has been decisive in the structure determinations.[1-3]

Alternatively, supported organometallic species analogous to molecular structures are attractive as model supported metal catalysts offering several advantages with respect to fundamental understanding of structure and performance: (1) the structure can, in prospect, be determined with precision, on the basis of comparisons of sample spectra and those of fully characterized molecular analogues; (2) the nature of the bonding between the organometallic species and the support can be determined with precision on the basis of comparisons of specta of surface species with those of analogous molecular structures incorporating ligands similar to those of the functional groups terminating the support surface. Therefore, the often ill-defined issues related to the structure of supported metal catalysts and metal–support interactions can be placed on a firm fundamental foundation.

The supported "molecular" organometallics that have been characterized most thoroughly are triosmium clusters anchored to silica and to alumina.[4-9] The structure has been inferred to

* To whom correspondence should be addressed.
† Eindhoven University of Technology.
‡ University of Delaware.

(1) Van Zon, J. B. A. D.; Koningsberger, D. C.; Van 't Blik, H. F. J.; Sayers, D. E. *J. Chem. Phys.* **1985**, *82*, 5742.
(2) Via, G. H.; Sinfelt, J. H.; Lytle, F. W. *J. Chem. Phys.* **1979**, *71*, 690.
(3) Sinfelt, J. H.; Via, G. H.; Lytle, F. W.; Greegor, R. B. *J. Chem. Phys.* **1981**, *75*, 5527.
(4) Psaro, R.; Ugo, R. *Metal Clusters in Catalysis*; Gates, B. C., Guczi, L., Knözinger, H., Eds.; Elsevier: Amsterdam, in press.
(5) Psaro, R.; Ugo, R.; Zanderighi, G. M.; Besson, B.; Smith, A. K.; Basset, J. M. *J. Organomet. Chem.* **1981**, *213*, 215.
(6) Deeba, M.; Gates, B. C. *J. Catal.* **1981**, *67*, 303.
(7) Knözinger, H.; Zhao, Y. *J. Catal.* **1981**, *71*, 337.
(8) Deeba, M.; Streusand, B. J.; Schrader, G. L.; Gates, B. C. *J. Catal.* **1981**, *69*, 218.

0002-7863/86/1508-6254$01.50/0